Simulations of detonation wave reflection over cylindrical convex surfaces with a detailed reaction model

Lisong Shi (時立松),¹ Zijian Zhang (張子健),² E Fan (范鍔),^{1, a)} and Chih-Yung Wen (温志湧)^{1, b)}

The unsteady reflection of detonation waves over cylindrical convex surfaces is numerically investigated using a high-resolution adaptive mesh refinement technique combined with a detailed reaction mechanism. Results reveal that cellular instabilities complicate the determination of the transition point from regular reflection to Mach reflection. However, the triple-point trajectories connecting the incident detonation wave and Mach stem remain largely unaffected by these instabilities. This consistency is confirmed by reducing the radius and the initial angle of the cylindrical surfaces. Finally, no universal scaling is observed across all configurations. At larger radii, the triple-point trajectories tend to stay closer to the surface.

When a detonation wave impinges on a solid wedge, either regular reflection (RR) or irregular/Mach reflection (MR) may occur, depending on the wedge angle. Numerous studies have explored these detonation reflection phenomena. 1-4 The irregular reflection of inert shock waves typically involves at least three shock waves. 5,6 Detonation waves, however, involve multiple transverse waves and possess finite characteristic thicknesses and non-uniform state distributions, which further complicate their irregular reflections. Specifically, Yang et al. reported the formation of a regular rhombic pattern, resulting from the intersection of incident transverse waves and reverse transverse waves. Due to the characteristic scales in detonation, the MR of a detonation wave is no longer selfsimilar, differing from the behavior of inert shock waves.⁶ Initially, the reflection follows a frozen limit and eventually reaches an equilibrium limit at the far end.⁸ This phenomenon was further confirmed through numerical studies of the reflections of both Zel'dovich-von Neumann-Döring (ZND) detonation waves^{9,10} and cellular detonation waves. ¹¹ Notably, the transition length between these two limits is much larger than the cellular length scale. Additionally, due to the presence of cellular detonation, stochastic variations in the triple-point origin have been observed near the apex of the wedge. 12

For detonation reflections on non-straight surfaces where the wall angle changes continuously, the phenomena are more complex than pseudo-steady reflections. Yuan *et al.*¹³ used a two-step induction-reaction model to analyze various parameters influencing detonation reflection over a cylindrical concave surface. They concluded that the ratio of induction to reaction zone length is a critical factor in the reflection process. Similarly, a numerical study of cellular reflection over a concave corner identified the critical angle for transition, which is significantly larger than that for a straight wedge.¹⁴ Detonation reflections over coupled convex-straight surfaces were found to delay the MR.¹⁵ Further studies on double-wedge reflections have identified seven kinds of reflection processes.¹⁶ Li and Ning¹⁷ conducted a systematic experimental and numerical study on detonation reflection over a cylindrical con-

Detonation reflections over cylindrical surfaces can be influenced by cellular instability, complicating direct investigations using detailed chemical mechanisms. This challenge arises because a well-established cellular detonation typically requires long propagation distances, and simulations often need to cover domain heights that span multiple detonation cells to ensure meaningful results in reflection problems. Consequently, this creates a significant computational challenge, especially when coupled with multi-species reaction models. The existing literature cited above, along with others, primarily relies on simplified two-step models or concentrates on limited spatial regions. Meanwhile, previous research has shown that the initial wall angle at the apex does not affect the transition for inert shock waves. 18 While earlier studies have predominantly concentrated on detonation reflections over half-cylindrical surfaces, there remains a notable gap in the literature regarding detonation reflections on cylindrical convex surfaces with reduced initial angles. This study aims to leverage the adaptive mesh refinement technique coupled with a detailed reaction model to numerically quantify the transition from RR to MR (RR \rightarrow MR) of cellular detonation waves propagating over cylindrical convex surfaces, with a particular focus on the global patterns observed for different radii and initial wall angles.

The multi-species reactive Euler equations are solved using the detailed chemical mechanism for high-pressure hydrogen combustion from Burke *et al.*¹⁹ A specific gas mixture of $2H_2 + O_2 + 3Ar$ is considered, exhibiting regular detonation cellular structures. The initial pressure is set to 0.25 atm, and the temperature is fixed at 300 K. The computational domain spans $[-20 \text{ cm}, 10 \text{ cm}] \times [0 \text{ cm}, 10 \text{ cm}]$, with an initial mesh of 1152×384 , resulting in a root mesh resolution of $\Delta x = \Delta y = 0.26$ mm. The initial wall angle at the apex of the cylindrical surface, as shown in Fig. 1, can be adjusted by offsetting the cylindrical surface by a distance of ΔH . Detonation is initiated by perturbed hot spots near the left end of the domain, traveling up to 20 cm until the detonation wave

¹⁾Department of Aeronautical and Aviation Engineering, The Hong Kong Polytechnic University, Kowloon, Hong Kong, China

²⁾School of Aerospace Engineering, Beijing Institute of Technology, Beijing, China

vex surface, observing scattering of the critical wall angle due to cellular instabilities through experiments. Furthermore, in the limit where the cell size is much smaller than the cylindrical radius, the critical wall angle approaches the inert two-shock theory.

^{a)}Corresponding author: e.fan@connect.polyu.hk

b) Corresponding author: chihyung.wen@polyu.edu.hk

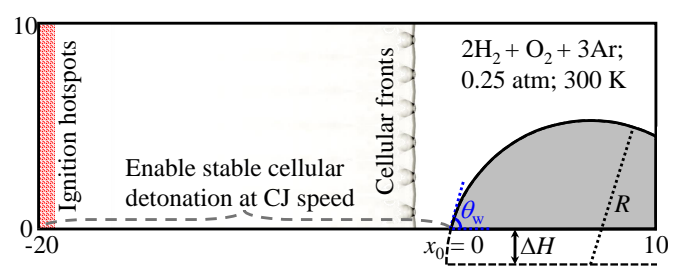


FIG. 1. Schematic of computational setup, the unit of length is cm.

TABLE I. Summary of test conditions. R represents the radius of the cylindrical surface, and $L \approx 0.83$ cm represents the cell length.

No.	1	2	3	4	5	6	7	8	9	10	11	12
<i>R</i> [cm]	7				3.5				1.75			
ΔH	0	0	R/2	R/2	0	0	R/2	R/2	0	0	R/2	R/2
x_0	0	L/2	0	L/2	0	L/2	0	L/2	0	L/2	0	L/2

reaches stable propagation at a velocity of 1869.1 m/s, which is close to the Chapman-Jouguet (CJ) velocity of 1871.4 m/s computed by the CEA (Chemical Equilibrium with Applications) code, ²⁰ with fully developed cellular structures before impacting the cylindrical convex surfaces.

To ensure high computational fidelity, adaptive mesh refinement (AMR) is employed to concentrate mesh resolution near the detonation fronts. The block-structured AMR solver for combustion, PeleC,²¹ is utilized in this study. The piecewise parabolic method (PPM)²² is used to reconstruct values at the cell faces, while an iteratively coupled scheme based on the spectral deferred correction (SDC) approach²³ is applied to advance the system through each numerical time step. Slip wall boundary conditions are applied to all surfaces. In the following simulation, five levels of refinement are used, with each refinement factor set to 2, yielding an effective mesh size of 8.138 μ m. The chosen resolution provides approximately 28 mesh points per detonation reaction zone induction length (28 pts/ l_{ind}). A separate convergence study was conducted indicating that doubling the resolution does not affect the detonation cell size ($\lambda \approx 0.455$ cm for cell width, $L \approx 0.83$ cm for cell length).

The test conditions for all cases are summarized in Table I. A total of three groups of cases are simulated, each representing a particular radius. Within each group, four cases are considered, with variations in the starting apex location and initial wall angle. The shift in the starting apex location x_0 , achieved by moving the cylindrical surface to the right by half the detonation cell length, enables the examination of cellular instability's impact on reflection phenomena. The starting angle is adjusted by lowering the cylindrical surface's center by half the radius, changing the initial wall angle ($\theta_{\rm w}$) from 90° to 60°. As will be shown later, with a starting angle of 60°, RR will continue to occur initially on the cylindrical convex surface. The cylindrical surface is implemented using the embedded boundary technique, and the adapted meshes are clustered around both the cylindrical surface and the detonation fronts, as shown in Fig. 2. All computations are performed on the Tianhe supercomputer at Tianjin Supercomputer Center, China.

To begin with, we first investigate the reflection of a detonation wave over a half-cylindrical surface with a radius of 7 cm

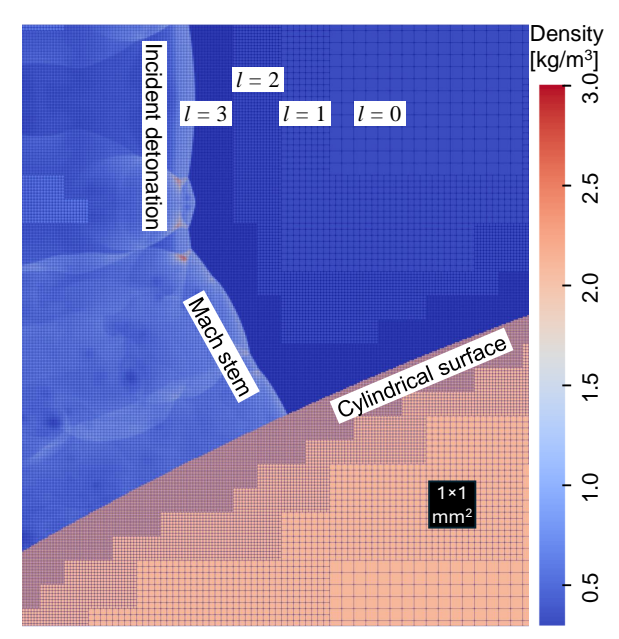


FIG. 2. Illustration of the adapted mesh near the reflected detonation waves at the cylindrical surface. For clarity, only three of the five refinement layers are shown.

and apex at x = 0 (Case 1). This radius spans approximately 15.4 detonation cell widths (i.e., $R/\lambda = 15.4$), meaning the detonation's characteristic scale is significantly smaller than that of the surface. The initial wall angle is sufficiently large to produce a RR. As the wall angle gradually decreases, the reflection eventually becomes irregular. The wave structures near the critical time for the $RR \rightarrow MR$ transition are shown in Fig. 3. Initially, when the detonation wave impinges on the curved surface, a RR is formed due to the large angle near the apex, as observed at $t = 108 \ \mu s$ and $t = 111 \ \mu s$. MR is observed at $t = 112.5 \mu s$, although it is difficult to confirm whether this can be considered a global structure (in terms of a formal MR of the incident detonation wave), given the substantial variations in cellular fronts and local velocity. Previous studies on inert (and planar) shock reflection over cylindrical surfaces have noted that determining the exact transition point is non-trivial, as the growth rate of the Mach stem at the onset of the transition is extremely small. This can lead to errors in extrapolation, beyond the capabilities of current experimental methods.⁵ Identifying the first appearance of the Mach stem has proven difficult, ^{24,25} and a similar observation is anticipated for detonation reflections, possibly more complex due to the stronger transverse instabilities compared to planar inert shocks.

At $t=114~\mu s$, the height of the Mach stem is significantly reduced, revealing stochastic local reflection patterns due to cellular instabilities. Subsequently, at $t=115.5~\mu s$ and $t=118.5~\mu s$, the height of the Mach stem gradually increases, a typical MR process over convex surfaces which aligns with findings from previous experimental studies. At the initial stage of MR, the Mach stem is significantly overdriven, where "overdriven" refers to the wave propagation speed exceeding the CJ velocity. The downstream-propagating transverse waves reflected from the convex surface, forming the rhombic pat-

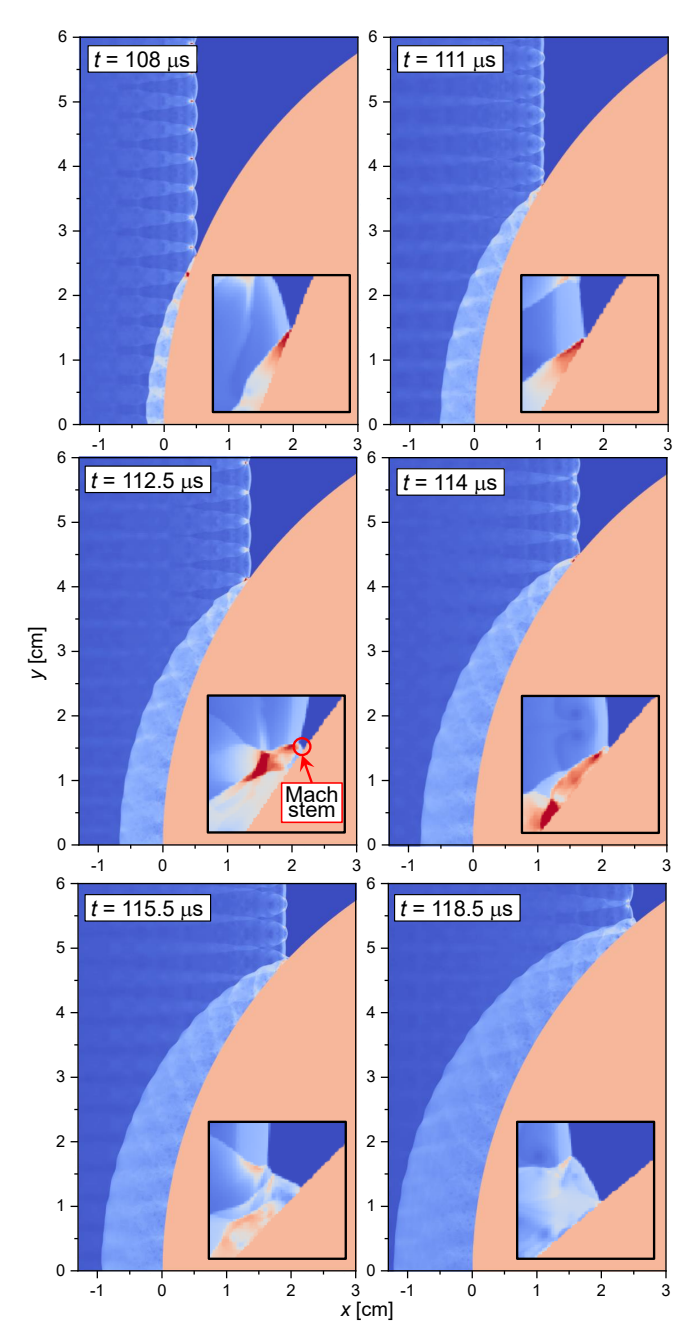


FIG. 3. Density contour plots illustrating the transition from RR to MR for Case 1. The color bar is the same as that in Fig. 2. Note that the time intervals between these plots are not uniform.

tern described in Yang *et al.*⁷ Based on these observations, the RR \rightarrow MR transition can be considered to occur somewhere between 111 μ s and 115.5 μ s.

It is crucial to note that, even near the transition point, the reflected shock wave is not perpendicular to the incident detonation wave. This is in variance with the transition criterion for inert shock waves over convex surfaces proposed by Geva et al., ²⁶ emphasizing the fundamental differences between RR \rightarrow MR transitions in detonations and inert shock waves. This could be due to the thermochemical non-equilibrium of the reflected shock, where the state behind the reflected shock experiences significant heat release (the mixture is rapidly burned

behind the reflected shocks in Fig. 3). Further investigation is needed, possibly with a detailed examination of the unsteady reflection of a ZND planar detonation wave.

Based on the findings above, it has been shown that determining the transition point from transient plots is neither straightforward nor accurate. Therefore, the transition point is directly determined from the numerical soot foil, though there may still be errors on the order of a few pixels, making it difficult to definitively determine whether the Mach stem persists or diminishes. As a result, in some cases, multiple transition points may be provided. The corresponding numerical soot foil for Case 1 is shown in Fig. 4a. The small MR observed at $t = 112.5 \,\mu s$ is likely a local MR due to cellular instability, as denoted by θ_a in Fig. 4a. Continuous MRs begin at θ_b , approximately at $t = 114 \mu s$, as shown in Fig. 3. Additionally, two extra small dark zones are observed: one located before point a and the other between points a and b. Identifying the transition point from the soot foil seems straightforward in this case. It seems preferable to select point b as the RR \rightarrow MR transition point. However, as will be demonstrated in subsequent cases, determining the transition point can sometimes be challenging.

After the transition point, due to the cylindrical surface, the upward-traveling family of transverse waves clusters near the triple-point, while the downward-traveling family approaches the expanding boundary, causing the space to grow (Fig. 4a). This leads to smaller detonation cells farther from the surface and larger cells near the surface after the detonation wave passes over the top of the cylindrical surface. A similar phenomenon has been observed in previous experimental studies. ¹⁷ In the later stages, the top of the Mach stem begins to merge with the incident detonation wave.

It has been reported in experiments ¹⁷ that cellular instabilities lead to the scattering of critical angles. Therefore, it is essential to determine how sensitive the aforementioned reflection dynamics are to small changes in cellular patterns when the detonation wave impinges on the surface when using a detailed reaction model. In Case 2, the reflection occurs on a half-cylindrical surface, with the apex deliberately shifted downstream by half the detonation cell length. The overall phenomenon is similar to Case 1, so detailed transient plots of wave structures are omitted. The soot foil for Case 2 is shown in Fig. 4b, where the fluctuation of the initial dark regions caused by local MR due to cellular instability differs from Case 1. The transition point shifts slightly (from approximately $y = 4.511 \text{ cm} (49.93^{\circ}) \text{ in Case 1 to } y = 4.337 \text{ cm}$ (51.78°) in Case 2), resulting in a 1.85° difference in the transition angle. To maintain consistency, the transition angle in this study is defined as the last starting point after which the Mach stem becomes continuous.

Cases 3 and 4 were conducted to explore whether modifying the incident angle at the apex from 90° to 60° significantly affects the transition patterns. The choice of a 60° angle is based on observations from Cases 1 and 2, where the detonation wave still experiences RR near the apex (thus before the transition point). Moreover, this change in angle is sufficiently large (representing a 50% change in the height of the cylindrical surface) to potentially influence the transition, if any effect

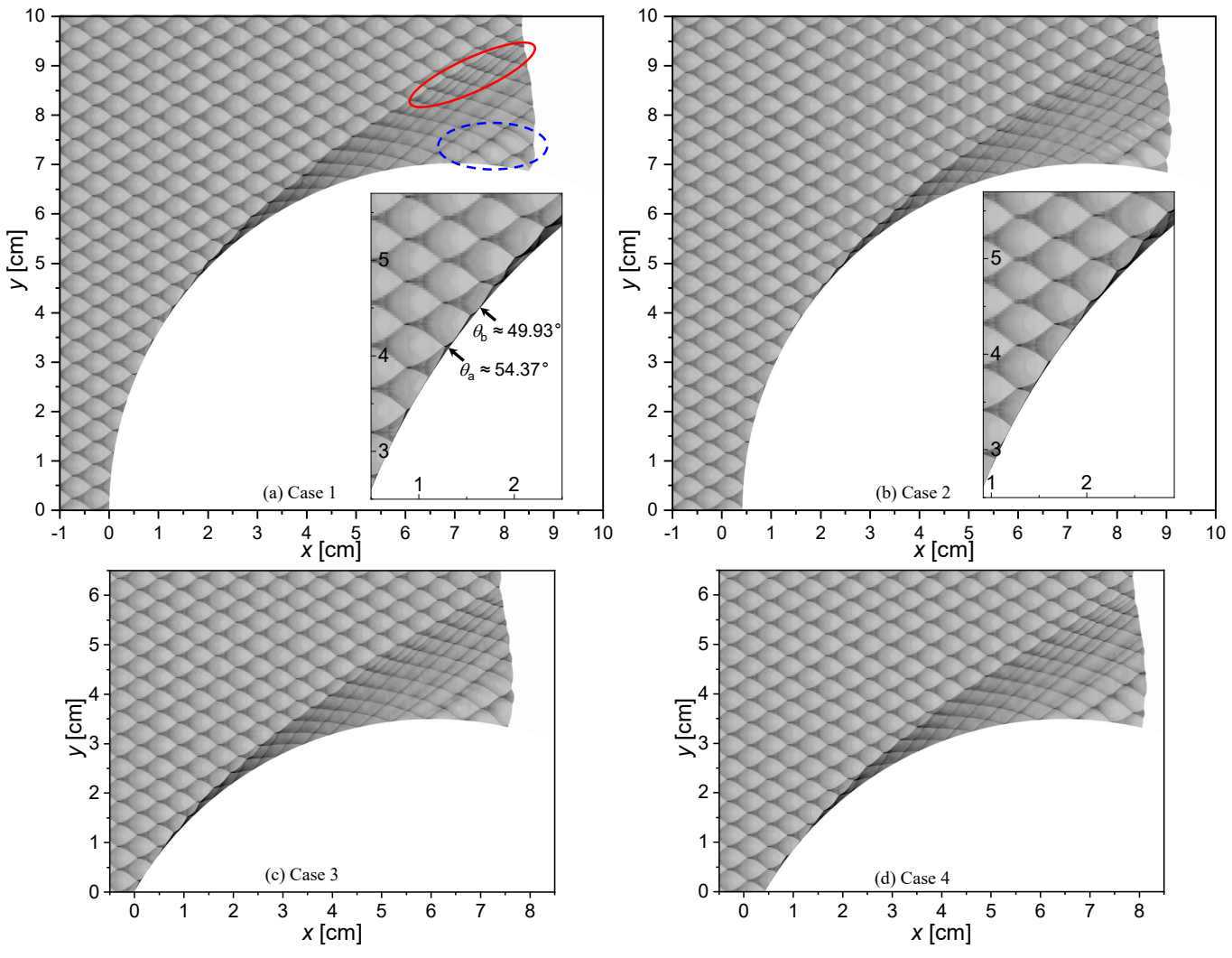


FIG. 4. Numerical soot foil for Cases 1–4, with a zoomed view near the transition point. θ_a and θ_b correspond to the locations of the detonation wave fronts $t = 112.5 \ \mu s$ and $t = 114 \ \mu s$, respectively. The red solid circle marks the small detonation cells clustered near the triple-point, while the blue dashed circle highlights the large detonation cells near the expanding surface.

is present.

From Fig. 4c–d, the transition angles for Cases 3 and 4 are measured as 52.61° and 48.24°, respectively. However, the differences between these values appear to fall within the fluctuation range of cellular instabilities. Therefore, measuring the transition angle directly from soot foils remains challenging, even with a relatively large radius-to-cell size ratio. Determining transition angles for detonation waves on convex surfaces is somewhat subjective, typically done by visual inspection of the visible Mach stem from either numerical results or experimental soot foils. A comprehensive discussion on this issue, specifically for inert shock reflections, is provided in Kleine *et al.*⁵

To provide a more insightful comparison, we plotted the triple-point trajectories for Cases 1–4 on a single graph (Fig. 5a). Note that the terminology "triple-point trajectory" in the present study primarily refers to the main triple point connecting the incident detonation wave and the Mach stem due to the reflection over the convex surface, rather than the

triple-point typically associated with tracing the detonation cellular structures. For consistency, we adjusted the origins of the cylindrical surfaces for the shifted cases (Cases 2 & 4) and those with smaller starting angles (Cases 3 & 4) to overlap with the origin of the benchmark case (Case 1). It is observed that all four trajectories closely overlap, particularly for x < 7 cm. Beyond this point, the Mach stem decays, and the triple-point trajectory merges with an upward transverse wave, resulting in a slight deviation in the trajectory.

The velocity profiles along the cylindrical surface (Fig. 5b) further support this observation, showing that the Mach stem transitions from an overdriven detonation wave to a state closer to the CJ detonation wave at the top of the cylindrical surface. The oscillations in velocity are attributed to the cellular nature of the detonation waves near the surface. Notably, the velocity patterns for all four cases follow a similar trend.

These findings suggest that, although the measured transition angles may vary due to the inherent difficulties in ac-

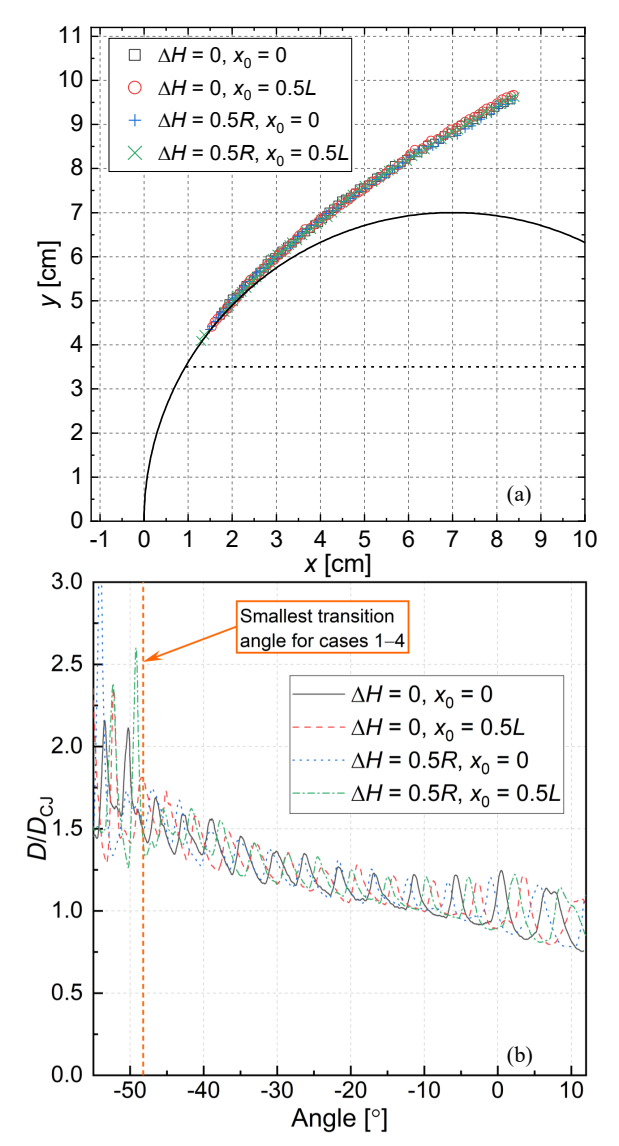


FIG. 5. (a) Trajectories of triple-points for Cases 1–4. To enable direct comparison, the origins of each plot have been adjusted such that the cylindrical surfaces overlap. The dashed line represents the lower wall for the partial cylindrical cases. Note that the first symbols of each case may not correspond to the start of the MR, as they could be influenced by local MRs induced by cellular instabilities. (b) Detonation wave velocity along the cylindrical convex surfaces. The angle of 0° corresponds to the top of the cylindrical surface.

curately determining the angle, the trajectories of the triple-points for a cylindrical convex surface with a specific radius do not differ significantly. This implies that selecting the triple-point trajectory as a measurable parameter may be more practical than relying on the transition angle, which can be influenced by experimental techniques, resolution limitations, and subjective factors. Furthermore, within the context of the present parameters and for cellular detonation wave reflection over a single cylindrical convex surface, the development of the MR pattern appears to be independent of the preceding history of RRs. The RR \rightarrow MR transition seems to be a local phenomenon, at least within the uncertainty caused by cellular instabilities.

The previous discussions focused on scenarios where the

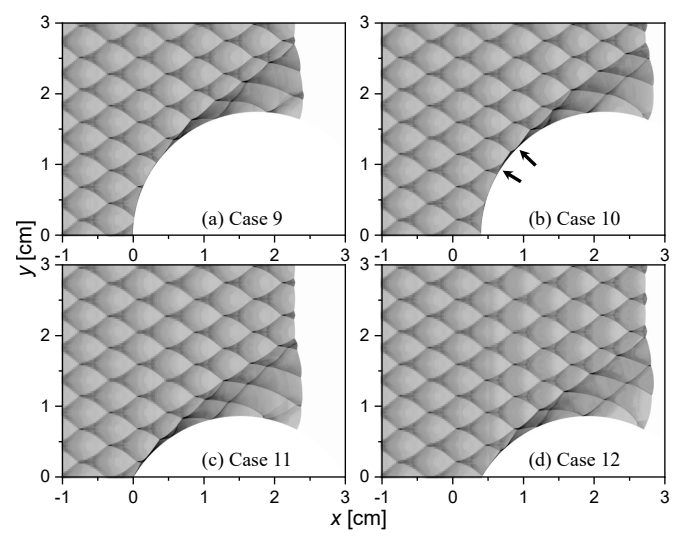


FIG. 6. Soot foils for cases 9–12. The two arrows in (b) illustrate the two possible determinations of the RR \rightarrow MR transition point. radius is significantly larger than the detonation cell size. Despite uncertainties in determining the transition angle, the trajectories of the triple points are closely aligned across different cases. The following will examine how the reflection behavior changes when the radius is reduced. Cases 5–8 and 9–12 test two sets of cases with smaller radii of 3.5 cm $(R/\lambda = 7.7)$ and 1.75 cm $(R/\lambda = 3.85)$, respectively.

The triple-point trajectories for cases with a radius of 3.5 cm remain tightly overlapped, resembling the behavior observed in previous instances with a large radius. However, for the 1.75 cm radius, the trajectories become less tightly aligned. This deviation can be attributed to the stronger influence of cellular instability at smaller radii, which only span 3.85 cell widths across the radius, as shown in Fig. 6. As discussed in cases 1–4, due to local variations in wave speed and wave angle near the transition point, the cellular front can induce local MRs, which are not a global phenomenon, and the Mach stem may even diminish at certain points. Consequently, the uncertainty in transition angles is more pronounced for surfaces with smaller radii, where the influence of cellular instability is much stronger. Furthermore, on the basis of case 9, two additional cases are considered. One case uses a refined mesh with an effective resolution of 56 pts/ l_{ind} to test mesh convergence, while the other solves the full set of reactive Navier-Stokes equations to examine viscous effects (Fig. 7). The results in Fig. 7 show almost no difference between these two cases and the original case in Fig. 6a. In the viscous case, the boundary layer behind the leading detonation wave is so thin that it has negligible influence on the final outcomes. Thus, the convergence of the present results is further confirmed, and viscous effects are deemed insignificant for the current study. However, these conclusions are based on the argon-diluted mixture, and further investigation may be needed for highly unstable detonations.

The velocity profiles (not shown here) along the surface follow a similar trend to those observed in cases 1–4, but with stronger fluctuations at the smaller radius. This is due to the larger changes in surface angle within one cellular structure at smaller radii. The transition angles for all cases are sum-

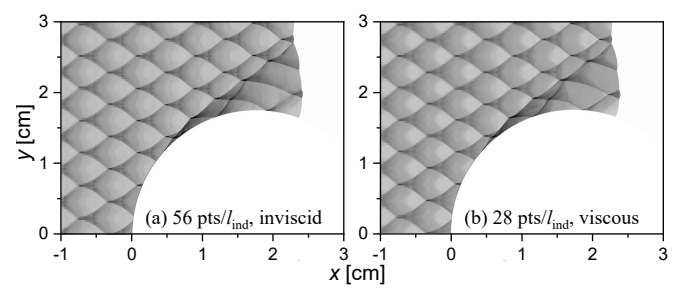


FIG. 7. Soot foils for case 9 variations: (a) with a refined mesh resolution that is half of the original, and (b) using the full set of reactive compressible Navier-Stokes equations.

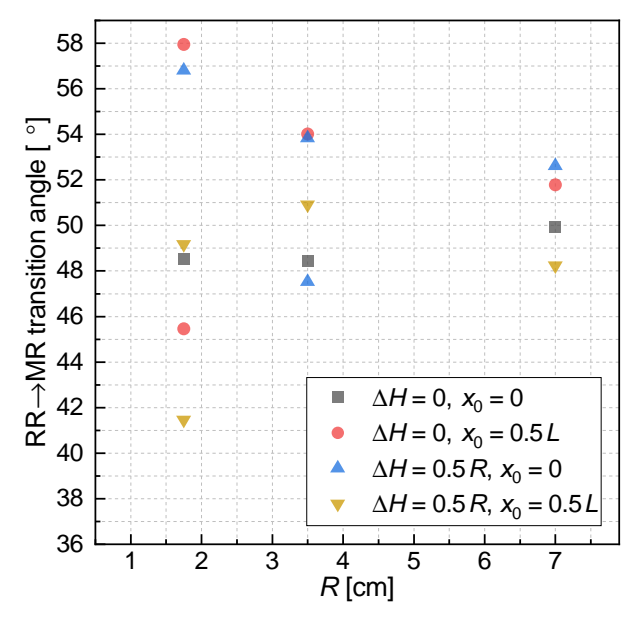


FIG. 8. Critical angles for all cases. Note that for R = 1.75 cm and R = 3.5 cm, some cases exhibit two critical angles. This occurs due to the challenges in precisely determining the critical angles, as seen in cases such as Case 10 in Fig. 6.

marized in Fig. 8. It is important to note that some cases are assigned two transition angles, reflecting the challenges in precisely determining the transition angle-particularly when the Mach stem height is so small that defining it accurately becomes difficult. An example of this is the shifted half-cylinder case (Case 10) shown in Fig. 6b. It is evident that determining the transition angle directly from either transient plots or soot foils can be somewhat ambiguous. This observation aligns with the experimental work on various types of mixtures by Li and Ning, ¹⁷ where scattering depends on the ratio of detonation cell size to the radius of curvature. As this ratio decreases, the scattering becomes significantly narrower. This behavior is also comparable to detonation reflection over a straight wedge: when the wedge length is similar to the cellular sizes, the problem becomes ill-defined. ¹¹

In light of the above interpretation, it is useful to investigate whether the Mach stem height scales with the cylindrical radius. To facilitate this, the trajectories are normalized by dividing by the corresponding radius, as shown in Fig. 9. The trajectories for cases with R=7 cm coincide with those for R=3.5 cm during the early stages after transition (zoomed-in view in Fig. 9). The trajectories for cases with R=1.75 cm

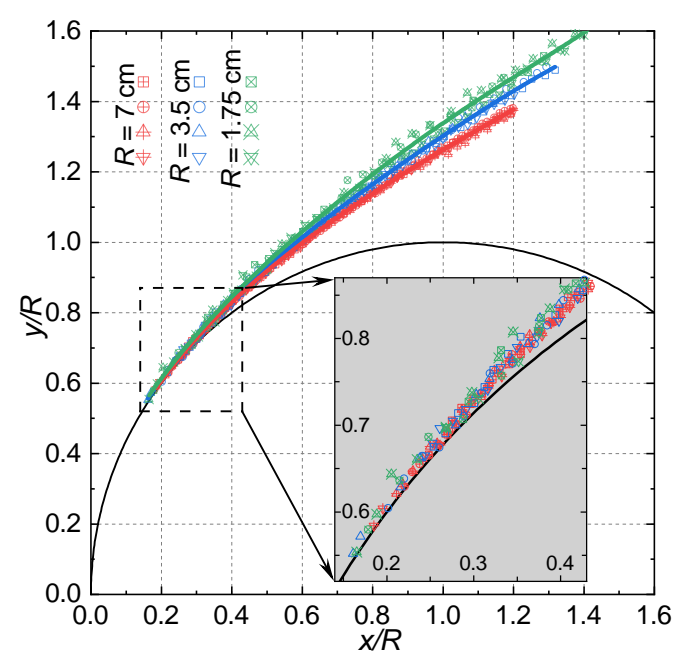


FIG. 9. Triple-point trajectories in the normalized dimension. The three solid curves represent the fitted trajectories for different radii. fluctuate around a similar path. However, as the MR progresses, the three groups of trajectories begin to diverge. As the radius decreases, the trajectory in the normalized dimension increases in height. Ultimately, all trajectories converge into traces of an upward-propagating transverse wave with the same angles. This indicates that the triple-point trajectories do not represent a scaling phenomenon.

In this letter, we focused on the numerical investigation of fully unsteady detonation reflection over a cylindrical convex surface, providing detailed insights into the transition phenomena from the fully established transition pattern. A stoichiometric hydrogen-oxygen mixture with 50% argon dilution, under initial conditions of 0.25 atm and 300 K, was examined. The adaptive mesh refinement technique made it possible to examine this problem at high-resolution over a large domain in terms of the radius-to-cell size ratio. It is important to note that for most cases, only inviscid simulations were performed, based on the assumption that viscous effects would be noticeable only for significantly small Reynolds numbers, or equivalently very small radii (approximately two orders difference in radii for inert shock reflection).⁵ A systematic study of viscous effects could be explored in future work. Cylindrical convex surfaces with three different radii, two different apex starting locations, and two different initial wall angles were tested in a total of 12 cases. The numerical results confirm a scatter in the transition angles from RR to MR, with the scatter becoming more pronounced for smaller radii. As a result, determining the effects of different radii, initial cellular perturbations, and starting apex angles on the transition angles is not immediately obvious, and some degree of arbitrariness may exist in this determination. Transition angles appear to be statistically meaningful only when the curvature radius is significantly larger than the characteristic length scales of detonation. Otherwise, the local and isolated MR due to cellular instabilities should be carefully taken into account in the investigation. Meanwhile, the triple-point trajectories have been shown to exhibit relatively consistent behavior, despite the influence of cellular instabilities.

Furthermore, it is important to re-emphasize that, for a constant radius, the RR \rightarrow MR transition appears to be independent of whether the starting angle at the apex is 90° or 60°. Despite the scattering caused by cellular instabilities, the triple-point trajectories for a specific radius overlap, suggesting that the trajectory is a more easily measurable phenomenon with potentially fewer human errors, at least compared to the influence of changing the radius. Finally, for the particular mixture tested in this study, all cases with different radii showed that, in the early stages of MR, the triple-point trajectories followed a similar path. However, in the later stages, this scaling similarity no longer holds. The non-selfsimilarity observed on cylindrical convex surfaces aligns with that seen in detonation reflection over straight wedges, 8,9,11 confirming the effect of finite length scales in detonation reflection phenomena. For larger radii, the triple-point trajectory is located closer to the cylindrical surface. Further studies on the unsteady reflection processes of ZND planar detonations and highly unsteady detonations with detailed reaction mechanisms are needed to provide a more comprehensive understanding of the reflection phenomena.

Acknowledgments

Zijian Zhang would like to recognize the financial support from the National Natural Science Foundation of China (No. 12202374). We express our gratitude to Wai Lee Chan for the valuable feedback on the manuscript and acknowledge the computing resources provided by the National Supercomputer Center in Tianjin.

AUTHOR DECLARATIONS

Conflict of Interest

The authors have no conflicts to disclose.

Author Contributions

Lisong Shi: Conceptualization; Formal analysis (lead); Data curation (equal); Software (equal); Writing – original draft (equal). **Zijian Zhang**: Data curation (equal); Funding acquisition (equal); Writing – review & editing (equal). **E Fan**: Formal analysis (supporting); Data curation (equal); Software (equal); Writing – original draft (equal). **Chih-Yung Wen**: Funding acquisition (equal); Writing – review & editing (equal); Supervision.

Data Availability Statement

The data that support the findings of this study are available from the corresponding author upon reasonable request.

- ¹R. Akbar, *Mach reflection of gaseous detonations* (Rensselaer Polytechnic Institute, 1997).
- ²S. Ohyagi, T. Obara, F. Nakata, and S. Hoshi, "A numerical simulation of reflection processes of a detonation wave on a wedge," Shock Waves **10**, 185–190 (2000).
- ³D. Chen, H.-H. Ma, and L.-Q. Wang, "Mach reflection of detonation wave on porous wall," Physics of Fluids 35 (2023).

- ⁴L. Wang and H. Ma, "Detonation wave reflection over a concave–convex cylindrical wedge," Shock Waves **34**, 285–289 (2024).
- ⁵H. Kleine, E. Timofeev, A. Hakkaki-Fard, and B. Skews, "The influence of reynolds number on the triple point trajectories at shock reflection off cylindrical surfaces," Journal of Fluid Mechanics **740**, 47–60 (2014).
- ⁶G. Ben-Dor and G. Ben-Dor, *Shock wave reflection phenomena*, Vol. 2 (Springer, 2007).
- ⁷Z. Yang, B. Zhang, and H. D. Ng, "Experimental observations of gaseous cellular detonation reflection," Proceedings of the Combustion Institute **40**, 105519 (2024).
- ⁸Y. Fortin, J. Liu, and J. H. Lee, "Mach reflection of cellular detonations," Combustion and Flame **162**, 819–824 (2015).
- ⁹J. Li, J. Ning, and J. Lee, "Mach reflection of a znd detonation wave," Shock Waves 25, 293–304 (2015).
- ¹⁰T. Jing, H. Ren, and J. Li, "Onset of the mach reflection of zel'dovich-von neumann-döring detonations," Entropy 23, 314 (2021).
- ¹¹J. Li and J. Lee, "Numerical simulation of mach reflection of cellular detonations," Shock Waves 26, 673–682 (2016).
- ¹²C. Wang and C. Guo, "On the influence of low initial pressure and detonation stochastic nature on mach reflection of gaseous detonation waves," Shock Waves 24, 467–477 (2014).
- ¹³ X. Yuan, J. Zhou, X. Mi, and H. D. Ng, "Numerical study of cellular detonation wave reflection over a cylindrical concave wedge," Combustion and Flame 202, 179–194 (2019).
- ¹⁴J. Li, J. Pan, C. Jiang, Y. Zhu, Y. Zhang, and A. O. Ojo, "Numerical investigation on cellular detonation reflection over wedges with rounded corner," Acta Astronautica 181, 503–515 (2021).
- ¹⁵J. Li, J. Pan, C. Jiang, Y. Zhu, and E. K. Quaye, "Numerical simulation of detonation reflections over cylindrical convex-straight coupled surfaces," International Journal of Hydrogen Energy 46, 32273–32283 (2021).
- ¹⁶J. Li, J. Pan, C. Jiang, X. Shi, Y. Zhu, and E. K. Quaye, "Numerical study on detonation reflections over concave and convex double wedges," International Journal of Hydrogen Energy 47, 17033–17044 (2022).
- ¹⁷J. Li and J. Ning, "Experimental and numerical studies on detonation reflections over cylindrical convex surfaces," Combustion and Flame 198, 130– 145 (2018).
- ¹⁸B. W. Skews and H. Kleine, "Shock wave interaction with convex circular cylindrical surfaces," Journal of Fluid Mechanics 654, 195–205 (2010).
- ¹⁹M. P. Burke, M. Chaos, Y. Ju, F. L. Dryer, and S. J. Klippenstein, "Comprehensive h2/o2 kinetic model for high-pressure combustion," International Journal of Chemical Kinetics 44, 444–474 (2012).
- ²⁰S. Gordon and B. J. McBride, Computer program for calculation of complex chemical equilibrium compositions and applications, Vol. 1 (National Aeronautics and Space Administration, Office of Management . . . , 1994).
- ²¹M. T. Henry de Frahan, J. S. Rood, M. S. Day, H. Sitaraman, S. Yellapantula, B. A. Perry, R. W. Grout, A. Almgren, W. Zhang, J. B. Bell, et al., "Pelec: An adaptive mesh refinement solver for compressible reacting flows," The International Journal of High Performance Computing Applications 37, 115–131 (2023).
- ²²P. Colella and P. R. Woodward, "The piecewise parabolic method (ppm) for gas-dynamical simulations," Journal of Computational Physics **54**, 174–201 (1984).
- ²³A. Nonaka, M. S. Day, and J. B. Bell, "A conservative, thermodynamically consistent numerical approach for low mach number combustion. part i: Single-level integration," Combustion Theory and Modelling 22, 156–184 (2018).
- ²⁴E. Timofeev, B. Skews, P. Voinovich, K. Takayama, G. Ball, R. Hillier, and G. Roberts, "The influence of unsteadiness and three-dimensionality on regular-to-mach reflection transitions: a high-resolution study," in *Shock waves, Proceedings of the 22th International Symposium on Shock Waves, London, UK* (1999) pp. 18–23.
- ²⁵H. Kleine, E. Timofeev, A. Gojani, M. Tetreault-Friend, and K. Takayama, "On the ongoing quest to pinpoint the location of rr-mr transition in blast wave reflections," in *Shock Waves: 26th International Symposium on Shock Waves, Volume 2* (Springer, 2009) pp. 1455–1460.
- ²⁶M. Geva, O. Ram, and O. Sadot, "The regular reflection → mach reflection transition in unsteady flow over convex surfaces," Journal of Fluid Mechanics 837, 48–79 (2018).